J. Inst. Eng. India Ser. C (July–September 2013) 94(3):213–223
DOI 10.1007/s40032-013-0076-y

ORIGINAL CONTRIBUTION

Mixed Convection with Conduction and Surface Radiation from a Vertical Channel with Discrete Heating

S. D. Londhe · C. G. Rao

Received: 13 May 2013 / Accepted: 23 August 2013 / Published online: 4 October 2013

Abstract A numerical investigation into fluid flow and heat transfer for the geometry of a vertical parallel plate channel subjected to conjugate mixed convection with radiation is attempted here. The channel considered has three identical flush-mounted discrete heat sources in its left wall, while the right wall that does not contain any heat source acts as a sink. Air, assumed to be a radiatively non-participating and having constant thermophysical properties subject to the Boussinesq approximation, is the cooling agent. The heat generated in the left wall gets conducted along it and is later dissipated by mixed convection and radiation. The governing equations, considered in their full strength sans the boundary layer approximations, are converted into vorticity-stream function form and are then normalized. These equations along with pertinent boundary conditions are solved through finite volume method coupled with Gauss-Seidel iterative technique. The effects of modified Richardson number, surface emissivity, thermal conductivity and aspect ratio on local temperature distribution along the channel, maximum channel temperature and relative contributions of mixed convection and radiation have been thoroughly studied. The prominence of radiation in the present problem has been highlighted.

Keywords Mixed convection · Conduction · Radiation · Interaction · Vertical channel · Discrete heat sources

List of Symbols

AR	Aspect ratio, L/W
A_{r1}, A_{r2}	Geometric ratios, W/t and W/L_h, respectively
$\bar{C}_f$	Mean friction coefficient
F_{ik}	View factor from the ith element to kth element of an enclosure
Gr_w^*	Modified Grashof number, $[(g\beta\Delta T_{ref}W^3)/\nu_f^2]$
g	Acceleration due to gravity, 9.81 m/s^2
J_i	Radiosity of a given element i of the enclosure, W/m^2
J_i'	Non-dimensional radiosity of a given element i of the enclosure, $[J_i/(\sigma T_\infty^4)]$
k_f	Thermal conductivity of air, W/m K
k_s	Thermal conductivity of channel wall as well as heat source, W/m K
L, L_h	Heights of channel wall and heat source, respectively, m
M_1	Grid number at the top end of the first heat source in the wall
M_2	Grid number at the bottom end of the second heat source in the wall
M_3	Grid number at the top end of the second heat source in the wall
M_4	Grid number at the bottom end of the third heat source in the wall
M_5	Total number of grids along the wall
M, N	Total number of grids in X and Y directions, respectively
n	Total number of elements of the enclosure
N_{RF}	Radiation-flow interaction parameter, $[\sigma T_\infty^4/(k_f\Delta T_{ref}/W)]$
Pe_w	Peclet number based on the width of the channel, $[Re_wPr]$ or $[u_\infty W/\alpha]$
Pr_f	Prandtl number of air, $[\nu_f/\alpha]$
$q_{cond,x,in}$	Conduction heat transfer into an element along the wall, W
$q_{cond,x,out}$	Conduction heat transfer out of an element along the wall, W

S. D. Londhe · C. G. Rao (✉)
Department of Mechanical Engineering, National Institute of Technology, Warangal 506 004, AP, India
e-mail: cgr_gcr@yahoo.co.in

q_{conv} Convection heat transfer from an element of the wall, W
q_{gen} Heat generated in an element of the wall, W
q_{rad} Radiation heat transfer from an element of the wall, W
q_v Rate of volumetric heat generation in each discrete heat source, W/m^3
Re_w Reynolds number based on the width of the channel, $[u_\infty W/\nu_f]$
Ri_w^* Modified Richardson number based on the width of the channel, $[g\beta\Delta T_{ref} W/u_\infty^2]$ or $[Gr_w^*/Re_w^2]$
T Local temperature in the computational domain, K or °C
T_{max} Maximum temperature in the computational domain, K or °C
T_∞ Free stream temperature of air, K or °C
u, v Vertical and horizontal components of velocity, respectively, m/s
u_∞ Free stream velocity of air, m/s
U Non-dimensional vertical velocity of air, $[u/u_\infty]$ or $[\partial\psi/\partial Y]$
V Non-dimensional horizontal velocity of air, $[v/u_\infty]$ or $[-\partial\psi/\partial X]$
W Width or spacing of the channel, m
x, y Vertical and horizontal distances, respectively, m
X, Y Non-dimensional vertical and horizontal distances, x/W and y/W, respectively

Greek Symbols

α Thermal diffusivity of air, m^2/s
β Isobaric cubic expansivity of air, $[-(1/\rho)(\partial\rho/\partial T)_p]$, K^{-1}
γ Thermal conductance parameter, $[k_f W/(k_s t)]$
ε Surface emissivity of the walls of the channel
θ Non-dimensional local temperature, $[(T-T_\infty)/\Delta T_{ref}]$
θ_{av} Non-dimensional average temperature, $\left[\frac{1}{AR}\int_0^{AR}\theta(X)dX\right]$
θ_{max} Non-dimensional maximum temperature
ν_f Kinematic viscosity of air, m^2/s
σ Stefan-Boltzmann constant, 5.6697×10^{-8} W/m^2 K^4
ψ Non-dimensional stream function, $[\psi'/(u_\infty W)]$
ψ' Stream function, m^2/s
ω Non-dimensional vorticity, $[\omega' W/u_\infty]$
ω' Vorticity, s^{-1}

Miscellaneous Symbols

Δx_{hs} Height of the element in the heat source portion of the wall
ΔX_{hs} Non-dimensional height of the element in the heat source portion of the wall
ΔT_{ref} Modified reference temperature difference, $[q_v L_h t/k_s]$, K or °C

Introduction

The fluid flow and heat transfer vis-à-vis the geometry of a vertical channel have been studied analytically, numerically as well as experimentally by several researchers. The experimental results of free convection in a vertical, symmetrically heated, isothermal channel with air as the cooling medium were reported by Elenbass [1]. Agrawal [2] used variational method to study combined free and forced convection in a vertical rectangular channel. Bar-Cohen and Rohsenow [3] developed composite relations for the variation of heat transfer coefficient along the channel subjected to natural convection for both symmetric and asymmetric isothermal (or isoflux) boundary conditions. Aung and Worku [4] provided numerical results for the effect of buoyancy on both hydrodynamic and thermal parameters concerning laminar and vertically upward mixed convection flow of a gas in a parallel-plate channel.

Carpenter et al. [5] have probed, numerically, the interaction of surface radiation with developing laminar free convection between two vertical plates with asymmetric but uniform heat fluxes. Sparrow et al. [6] reported numerical results for the problem of combined radiation and developing free convection in a vertical channel equipped with one isothermal wall and one adiabatic wall and claimed a 50–70 % enhancement in heat transfer on considering the effect of radiation. Laminar forced convection heat transfer between a series of parallel plates with surface mounted heat source blocks is tackled numerically by Kim and Anand [7]. Gururaja Rao et al. [8] solved the problem of two-dimensional conjugate laminar mixed convection with radiation from a vertical plate with a single flush-mounted discrete heat source. Gururaja Rao et al. [9] have made a detailed probe into conjugate mixed convection with surface radiation from a vertical channel equipped with a flush-mounted discrete source in each of its walls.

Bhowmik and Tou [10] studied, experimentally, convective heat transfer in a vertical rectangular channel containing an array of four in-line square chips that are flush-mounted on one of its walls, cooled with laminar water flow under free, mixed and forced convection conditions. Sawant and Gururaja Rao [11] numerically studied the problem of conduction-mixed convection-radiation from a vertical plate with three identical flush-mounted discrete heat sources. Aminossadati and Ghasemi [12] investigated, numerically, mixed convection heat transfer in a two dimensional horizontal channel with a discrete heat source located on one of its walls. A numerical investigation on laminar free convection in a vertical channel with asymmetric heating has been performed by Terekhov and Ekaid [13]. Sun et al. [14] performed numerical simulation studies on mixed convection of air between vertical isothermal

plates and tried to determine the optimum spacing pertaining to the peak heat flux that is transferred from an isothermal parallel-plate array being cooled by mixed convection. Sakurai et al. [15] probed into the effects of radiation on turbulent mixed (free and forced) convection in a horizontal channel through direct numerical simulation. Al-Amri and El-Shaarawi [16] reported the effect of surface radiation on the developing laminar mixed convection flow of a transparent gas through an asymmetrically heated vertical parallel-plate channel and presented threshold values of emissivity at which one can ignore radiation effects. El-Morshedy et al. [17] presented the heat transfer characteristics pertaining to natural convection in a vertical rectangular channel that simulates the cooling channel of a typical material testing reactor based on their experimental observations. Li et al. [18] documented numerical solutions regarding the effect of surface radiation on laminar air flow taking place in a vertical and asymmetrically-heated channel. Dritselis et al. [19] worked on the influence of a spatially periodic temperature boundary condition on the laminar mixed convection involving an upward flow occurring between two vertical parallel plates.

A comprehensive study of the literature pertaining to the channel geometry subjected to multi-mode heat transfer (free, forced or mixed convection, conduction and radiation) hints at the need to take up exhaustive parametric studies on conjugate mixed convection with radiation from a discretely heated vertical channel. Owing to this, a numerical investigation into interaction of radiation with conjugate mixed convection from a vertical channel possessing three identical and flush-mounted discrete heat sources in its left wall is taken up in the present paper. The governing fluid flow and heat transfer equations are handled in their full strength without assuming fully developed flow and without the boundary layer approximations. A computer code is exclusively written to solve these equations through finite volume method in conjunction with Gauss-Seidel solver.

Description and Formulation of the Problem

The geometry of a vertical parallel-plate channel with multiple heat sources in the left wall, along with the discretized computational domain and pertinent boundary conditions, is shown in Fig. 1. The height and the thickness of both the channel walls are L and t ($\ll$ L), respectively, while they are separated by a distance W called channel width (or spacing). For a given height L, the aspect ratio (AR) is defined as L/W such that a smaller AR represents larger channel width, while a larger AR denotes smaller channel width. The thermal conductivity of the channel walls is k_s and the emissivity of their inside surfaces is ε. The outer, top and bottom surfaces of both the channel walls are adiabatic. There are three identical flush-mounted discrete heat sources, each of height L_h, provided in the left wall, while the right wall does not possess any heat source. The volumetric heat generation in each of the three heat sources, positioned at the bottom, center and top of the left wall, is q_v W/m^3. Air, assumed to be radiatively transparent and of constant thermophysical properties with the Boussinesq approximation being valid, is the cooling medium and it enters the channel from its bottom at a mean velocity u_∞ and temperature T_∞. The heat generated in the three heat sources of the left wall gets percolated through the wall by conduction, before getting dissipated by mixed convection and radiation. The right wall receives heat from the left wall by radiation that is later dissipated to air.

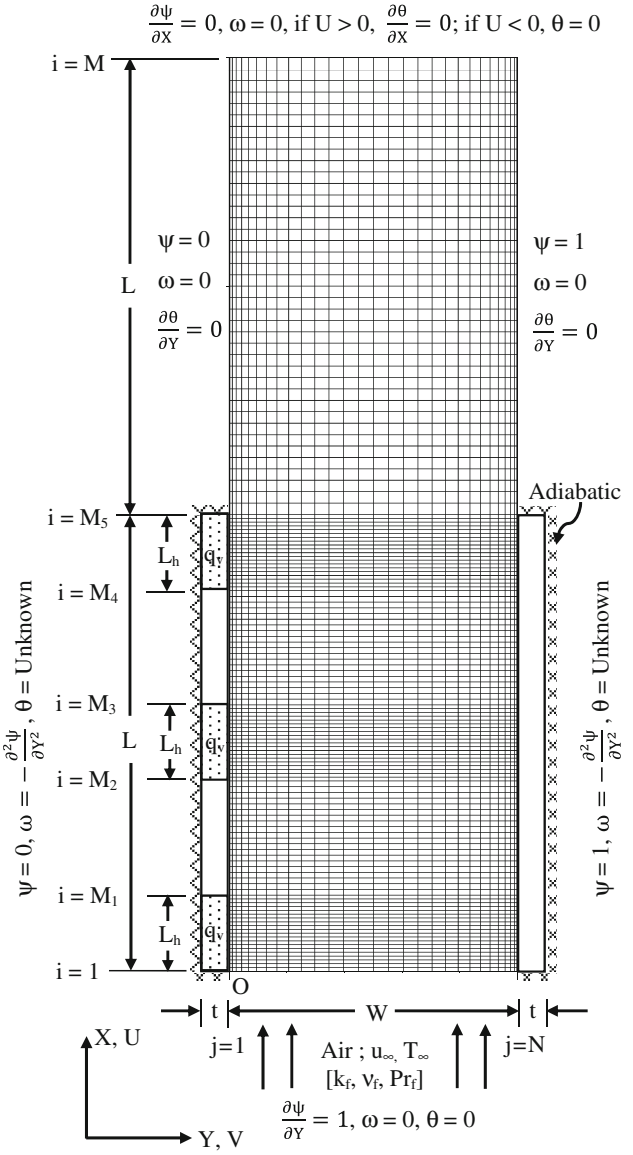

Fig. 1 Vertical channel chosen for study along with discretized computational domain and boundary conditions used

The governing equations pertaining to the present problem are the continuity equation, the x and y momentum equations and the equation of energy. These equations in primitive variables are first expressed in vorticity-stream function ($\omega - \psi$) form. The resulting vorticity transport equation, stream function equation and energy equation are normalized making use of the following set of non-dimensional parameters:

$$X = x/W,\ Y = y/W,\ U = u/u_\infty,\ V = v/u_\infty,$$
$$\psi = \psi'/(u_\infty W), \omega = (\omega' W)/u_\infty \text{ and}$$
$$\theta = (T - T_\infty)/\Delta T_{ref},$$

where $\Delta T_{ref} = (q_v L_h t)/k_s$

The final set of normalized equations would be:

$$U\ \frac{\partial \omega}{\partial X} + V\ \frac{\partial \omega}{\partial Y} = -Ri_w^* \frac{\partial \theta}{\partial Y} + \frac{1}{Re_w}\left(\frac{\partial^2 \omega}{\partial X^2} + \frac{\partial^2 \omega}{\partial Y^2}\right) \quad (1)$$

$$\frac{\partial^2 \psi}{\partial X^2} + \frac{\partial^2 \psi}{\partial Y^2} = -\omega \quad (2)$$

$$U\ \frac{\partial \theta}{\partial X} + V\ \frac{\partial \theta}{\partial Y} = \frac{1}{Pe_w}\left(\frac{\partial^2 \theta}{\partial X^2} + \frac{\partial^2 \theta}{\partial Y^2}\right) \quad (3)$$

The parameter, Ri_w^*, appearing in Eq. (1) is the modified Richardson number, defined as Gr_w^*/Re_w^2, which separates the flow into various regimes. A value of $Ri_w^* \approx 1$ indicates pure mixed convection, while a larger Ri_w^* represents asymptotic free convection, with a smaller Ri_w^* representing asymptotic forced convection.Equations (1–3) are solved along with the pertinent boundary conditions imposed on ψ, ω and θ. For the temperature boundary condition along the channel walls, appropriate energy balance is made considering the distinct elements. For example, energy balance on a typical element within the heat source portions of the left wall of the channel is:

$$q_{gen} + q_{cond,x,in} = q_{cond,x,out} + q_{conv} + q_{rad} \quad (4)$$

This, after substitution of component terms in it and subsequent simplification, gives:

$$k_s t \frac{\partial^2 T}{\partial x^2} + k_f \left(\frac{\partial T}{\partial y}\right)_{y=0} + q_v t - \frac{\varepsilon}{1-\varepsilon}\left[\sigma T_i^4 - J_i\right] = 0 \quad (5)$$

After appropriately normalizing, the above results in:

$$\frac{\partial^2 \theta}{\partial X^2} + \gamma\left(\frac{\partial \theta}{\partial Y}\right)_{Y=0} + A_{r1}A_{r2} - \frac{\varepsilon}{1-\varepsilon}\gamma N_{RF}\left[\left(\frac{T_i}{T_\infty}\right)^4 - J_i'\right] = 0 \quad (6)$$

Here, γ and N_{RF} indicate the thermal conductance parameter and the radiation-flow interaction parameter, respectively, with A_{r1} and A_{r2} referring to two of the non-dimensional geometric parameters. J_i' refers to non-dimensional radiosity of the ith element, given by $J_i/\sigma\ T_\infty^4$, where J_i is radiosity, which, in turn, is given by

$$J_i = \varepsilon\sigma T_i^4 + (1-\varepsilon)\sum_{k=1}^{n} F_{ik}J_k \quad (7)$$

where n is the total number of elements of the enclosure formed by the four boundaries of the computational domain. Hottel's crossed string method is used to compute the view factors needed in the above calculations. The energy balance on all other elements pertaining to the left wall and also the right wall is made using a similar treatment as above and the pertinent governing equations are evolved.

Solution Procedure and Parameters Employed

The normalized governing equations, viz., Eqs. (1–3), are converted to algebraic form using finite volume formulation and are solved through the Gauss-Seidel iterative method. Under relaxation, with a relaxation parameter 0.3, is used on vorticity (ω) as well as stream function (ψ), while full relaxation, with relaxation parameter unity, is used for temperature (θ). Convergence criteria that have been imposed on ψ, ω and θ are, respectively, 1×10^{-4}, 5×10^{-4} and 1×10^{-4}.

As shown in Fig. 1, an extended computational domain of height two times that of the channel wall is used to capture the fluid flow and heat transfer in the channel region correctly and completely. Since the temperature and velocity gradients are steeper near the walls, cosine grids, which are quite finer near the walls getting increasingly coarser towards the mid-plane of the channel, are selected across the channel (Y direction). Uniform grids of varying degree of fineness are employed along the height of the domain (X direction). The grids are quite finer in the heat source portions, slightly coarser in the non-heat source portions and still more coarser in the extended domain. The solution is obtained using a specifically written code in C^{++}. The solution gives the local velocities and temperatures at all the nodes in the entire computational domain. The maximum non-dimensional temperature (θ_{max}), the average non-dimensional temperature (θ_{av}) and the relative contributions of mixed convection and radiation are appropriately extracted using local values along the channel walls.

The channel height (L) is taken as 20 cm, while the thickness (t) of the wall is considered as 1.5 mm. The height (L_h) of each heat source is considered to be L/8 (2.5 cm). The range for AR is opted to be from 4 to 20, simulating, respectively, wider and narrower channels. The range for surface emissivity (ε) of each of the channel walls is taken to be 0.05–0.85. For thermal conductivity (k_s) of the channel, a range of $0.25 \le k_s \le 1$ W/m K is considered to be appropriate. For modified Richardson number (Ri_w^*), the

variation is between 0.1 and 25, which, respectively, stand for the asymptotic forced convection and the asymptotic free convection limits.

Results and Discussion

Grid Sensitivity Analysis

Before taking up the proposed exhaustive parametric study, it is customary to freeze the optimum grid system by carrying out a detailed grid independence test. The test is carried out in four stages over the range of the input of q_v, k_s, Ri_w^*, AR and ε. In the first stage, the number of grids (M_5) along the channel wall is varied by keeping the other grid sizes fixed and is freezed based upon the percentage change in the maximum non-dimensional temperature. Similarly, in the subsequent stages, the ratio of grid size in the heat source portion to that in the non-heat source portion of the left wall, the total number of grids in the X direction (M) and the number of grids across the channel (N) are fixed. It is concluded that the best grid system for the job is the one with $M \times N = 261 \times 61$, $M_1 = 25$, $M_2 = 79$, $M_3 = 103$, $M_4 = 157$ and $M_5 = 181$.

Testing the Results for Mass and Energy Balance

A check on the results of the present study has been made with regard to mass and energy balance in all regimes of mixed convection. On an average, it is observed that both the mass and energy balance are satisfactory with maximum deviations restricted, respectively, to ± 0.15 and ± 0.75 %.

Validation of Results

A study of non-dimensional vertical velocity and temperature profiles is made at the channel exit for a representative case that has a heat source in each wall with $q_V = 5 \times 10^5$ W/m^3, while k_s and ε are taken to be 0.5 W/m K and 0.45, respectively. Four different AR (4, 8, 16 and 20), covering the range ($4 \leq AR \leq 20$), have been considered. The study is carried out in the asymptotic forced convection limit ($Ri_w^* = 0.1$). It has been noticed that the flow even at the channel exit remains under developed for lower values of AR. Even for AR = 20, the velocity and temperature profiles have been found to be not merging with the fully-developed velocity and temperature profiles of plane-Poiseuille flow. Owing to these observations, the lowest AR (AR = 4) may be considered to be the flat plate limit implying that the two channel walls behave as though they are isolated from each other. Now, the validation of the fluid flow results is made by carrying out comparison of the mean friction coefficient ($\bar{C}_f$) calculation of the present work with the exact flat plate solution of Blasius in the asymptotic forced convection limit ($Ri_w^* = 0.1$). For this, fifteen data points are obtained for $Ri_w^* = 0.1$ with AR = 4. The $\bar{C}_f$ from the present work agreed well with that of Blasius with the maximum deviation limited to ± 7.8 %. Even a correlation has been deduced for $\bar{C}_f$ making use of the above 15 data that turned out to be: $\bar{C}_f = 1.382\, Re_L^{-0.5}$. This means a difference of ± 4.1 % between the present correlation and that of Blasius. Remembering that $Ri_w^* = 0.1$ is an asymptotic forced convection limit for the present problem with varying wall temperature and the Blasius solution was for forced convection past an isothermal flat plate, the above observations serve as validation for the fluid flow calculations of the present work.

In order to validate the heat transfer results, the present problem is simplified to the case that has the two channel walls remaining isothermal. A set of 18 data is obtained covering the entire AR range (AR = 4 to 20) for $Ri_w^* = 100$. The average convection Nusselt number obtained is compared with semi-empirical correlation of Elenbass [1] and the analytical solution of Bar-Cohen and Rohsenow [3], both of which are for free convection in air in a vertical channel with symmetric isothermal walls. An adequate parity is observed with maximum deviations limited to within ± 9.7 and ± 8.6 %, respectively.

Study of Local Temperature Profiles Along Channel Walls with Surface Emissivity

The variation of the local temperature distribution, T(x), along the left and the right walls of the channel is shown in Fig. 2a, b, respectively, for three different surface emissivities ($\varepsilon = 0.05$, 0.45 and 0.85). A fixed set of input parameters is used and it comprises $q_v = 1 \times 10^5$ W/m^3, $k_s = 0.25$ W/m K, AR = 12 and $Ri_w^* = 25$. Figure 2a indicates that, for a given ε, the local left wall temperature increases very sharply in the heat source portions with a subsequent drop in the non-heat source portions along the wall. Thus, three local maxima and two local minima are observed in the three heat source and two non-heat source portions, respectively. It is seen that the successive local maxima in T(x) are occurring in the ascending order with the overall maximum (T_{max}) occurring at the top adiabatic end of the wall. The waviness noticeable in the local temperature profiles is attributed to discrete heating adopted in the left channel wall. Further, it can be noted that, with increase in emissivity, the radiative dissipation from the left wall increases, which brings down the local left wall temperature. In the present case, for example, the third local peak along the wall decreases by 8.54 % as ε is increased to 0.85 from 0.05.

The effect of emissivity on right wall temperature distribution is depicted in Fig. 2b. A waviness is noticed in the local right wall temperature, for any given ε, which is due to a similar nature of variation of local left wall temperature distribution that has been discussed already. As emissivity

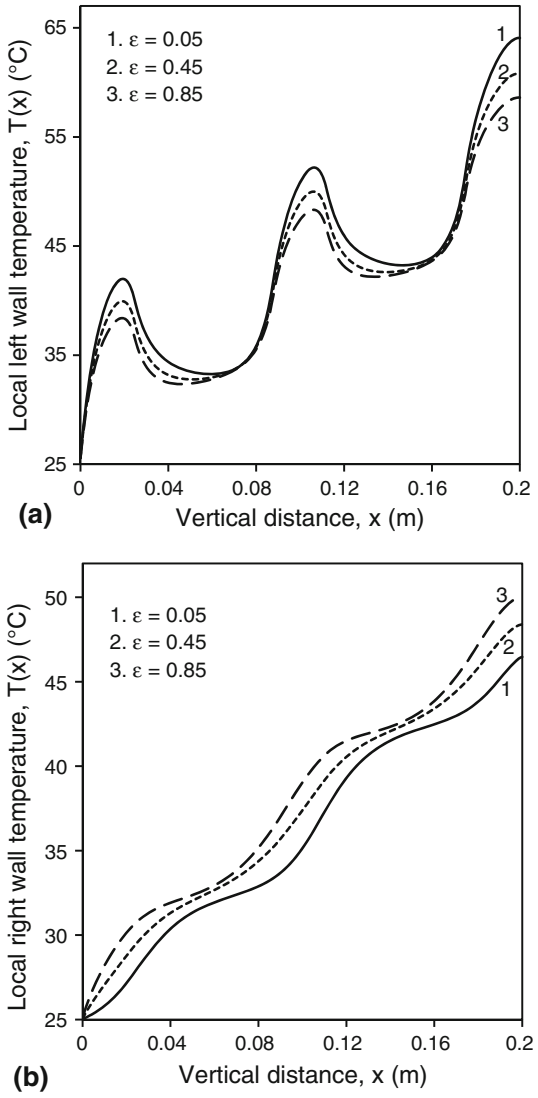

Fig. 2 Local *left* and *right* wall temperature profiles for different surface emissivities in a given mixed convection regime

increases, irradiation received by the right wall from the left wall significantly increases and as a consequence there is an increase in the local right wall temperature. In the present case, the local temperature at the top adiabatic end of the right wall increases by 7.64 % as ε is increased to 0.85 from 0.05.

Study of Variation of Local Temperature Distribution in Different Regimes of Mixed Convection

A study of variation of local temperature distribution along the left and right walls of the channel in different regimes of mixed convection is taken up for a given input as shown in Fig. 3a, b. Five typical values of modified Richardson number (Ri_w^*) are chosen to cater to the entire mixed convection regime from the asymptotic forced convection limit ($Ri_w^* = 0.1$) to the asymptotic free convection limit ($Ri_w^* = 25$). It is noticed that the general nature of variation of local temperature distribution either along the left or along the right wall of the channel is similar to that observed in Fig. 2a, b. Figure 3a clearly shows that there is a sharp decline in the local temperature along the left wall as the flow regime transits from free convection limit to pure mixed convection ($Ri_w^* = 1$), while the decline is mild as Ri_w^* subsequently changes to the forced convection limit. In the present study, T(x) at the exit of the channel along the left wall drops by 29.14 % as Ri_w^* decreases from 25 to 1, while for a further decrease in Ri_w^* to 0.1 from 1, T(x) at the same location decreases just by 10.16 %.

A similar trend is observed in the case of right wall temperature distribution as depicted in Fig. 3b. In the present example, at the exit of the channel, the right wall temperature decreases by 37.31 % as Ri_w^* decreases from 25 to 1, while it gets decreased only by 10.23 % as Ri_w^* further decreases to 0.1 from 1.

Study of Exclusive Effect of Surface Radiation on Local Temperature Distribution

An attempt is made to extract the exclusive role of surface radiation in deciding the local temperature distribution along the heat generating left wall of the channel. The study is carried out by considering two limiting values of emissivity, viz., $\varepsilon = 0$ signifying the case (1) without radiation and $\varepsilon = 0.99$ representing the case (2) with maximum possible radiation, which are conceivable with highly polished aluminum sheet and the lamp black soot, respectively. The temperature distribution is obtained for the fixed input of $q_v = 1 \times 10^5$ W/m^3, $k_s = 0.25$ W/m K, AR = 4 and $Ri_w^* = 25$, as shown in Fig. 4. It is observed that there is a substantial drop in local temperature along the left wall when once the highly reflecting and poorly emitting surface ($\varepsilon = 0$) is replaced by the best possible emitter ($\varepsilon = 0.99$). The drop in temperature is prominent in the heat source portions of the wall where greater temperature gradients are experienced. The above is attributed to the obvious augmentation of heat dissipation with increased surface emissivity (ε). For the present study, the temperature at the top adiabatic end of the left wall is noticed to be decreasing by 14.39 %. Thus, it is strongly advocated that radiation should be reckoned with while tackling the present kind of problems.

Study of Variation of Peak Channel Temperature with Surface Emissivity in Various Mixed Convection Regimes

Figure 5 shows interplay between surface radiation and mixed convection in influencing the peak channel

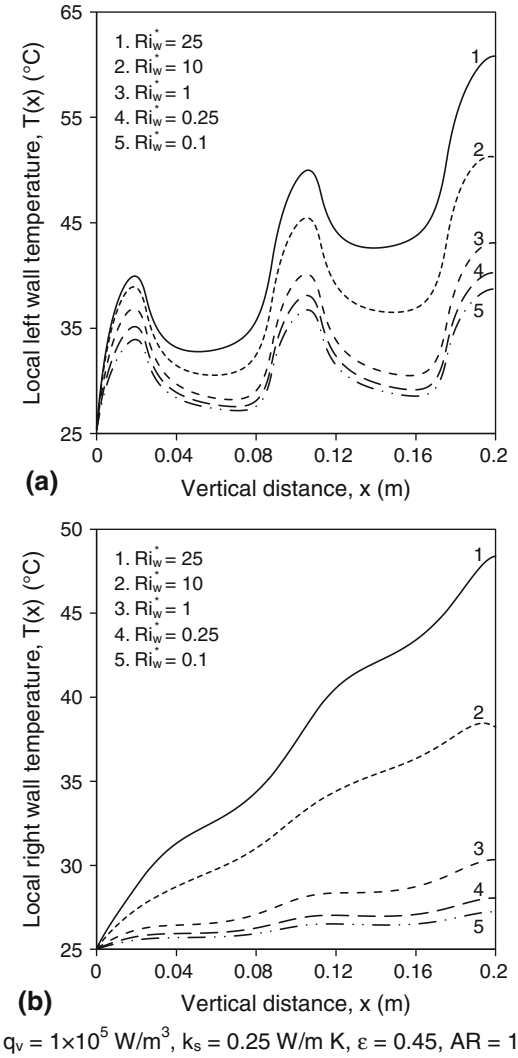

Fig. 3 Local *left* and *right* wall temperature profiles in different regimes of mixed convection for a given surface emissivity

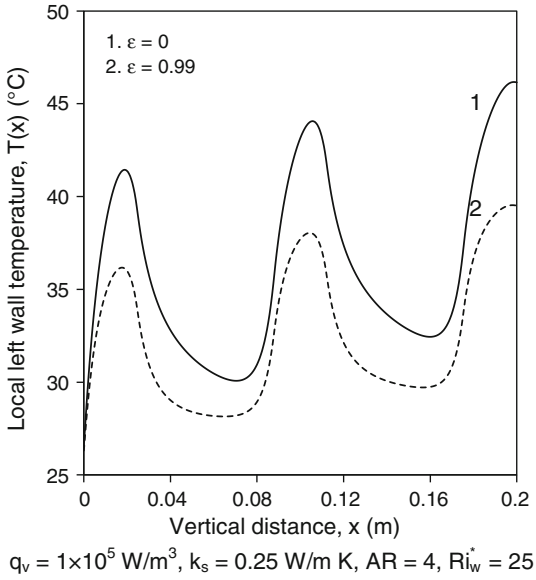

Fig. 4 Exclusive effect of radiation on local *left* wall temperature distribution

temperature (T_{max}) for a fixed set of input shown therein. Five values of ε are chosen, viz., 0.05, 0.25, 0.45, 0.65 and 0.85, while the curves are plotted for six values of Ri_w^* covering the entire mixed convection regime. The figure indicates that, for a given ε, T_{max} decreases with decreasing Ri_w^* owing to transition of the flow regime from free to forced convection resulting in increased rate of convection heat transfer. This effect is substantial in free convection dominant regime compared to forced convection dominant regime. In the present case, for ε = 0.45, T_{max} is found to be reducing by 39.34 % with Ri_w^* dropping from 25 to 1, while it reduces by a further 17.68 % with a subsequent drop in Ri_w^* to 0.1 from 1. The figure also reveals that T_{max} decreases monotonically with increasing ε for all values of Ri_w^*. This effect is more pronounced in the forced convection dominant regime compared to the free convection dominant regime. It is substantiated by the fact that radiative heat dissipation is increasing largely for $Ri_w^* = 0.1$ than for $Ri_w^* = 25$ as ε is increased from 0.05 to 0.85. In the present example, T_{max} is observed to decrease, respectively, by 8.94, 8.86 and 6.21 % for $Ri_w^* = 0.1$, 1 and 25 as ε is increased from 0.05 to 0.85.

Study of Effect of Surface Emissivity on Peak Channel Temperature for Different Channel Materials

The interactive effect of thermal conductivity (k_s) of the channel material and surface emissivity (ε) on the maximum temperature achieved by the channel is depicted in Fig. 6. The input values of other parameters being fixed for the study are also mentioned in the figure. A drop in T_{max} with increase in ε is observed, for a given k_s, due to increased radiative heat dissipation from the channel wall. This decrease in T_{max} is noticed to be smaller for larger values of k_s. In the present case, for $k_s = 0.25$ W/m K, T_{max} decreases by 10.54 % as ε increases to 0.85 from 0.05, while it drops down by 8.18 % for $k_s = 1$ W/m K. The figure further shows that, for a given ε, T_{max} increases with increasing k_s. The heat percolates at a faster rate with a gradual increase in k_s, thereby increasing T_{max} achieved by the channel. In the present example, for ε = 0.45, T_{max} increases by 5.74 % as k_s increases from 0.25 to 1 W/m K.

Study of Effect of Thermal Conductivity on Peak Channel Temperature in Various Mixed Convection Regimes

The variation of T_{max} with thermal conductivity (k_s) of the wall material in different regimes of mixed convection

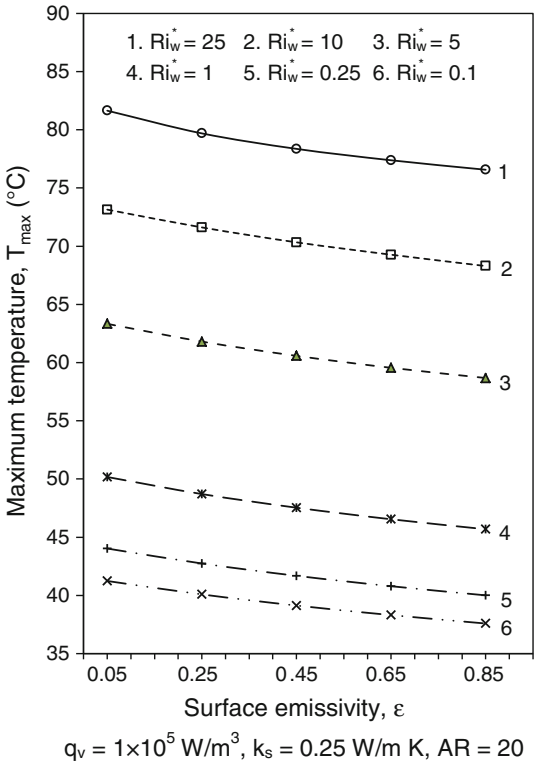

Fig. 5 Effect of surface emissivity on peak channel temperature in different mixed convection regimes

(five different values of Ri_w^*) is demonstrated in Fig. 7. The fixed input considered for study comprises $q_v = 1 \times 10^5$ W/m^3, $\varepsilon = 0.45$ and AR = 12. For a given k_s, T_{max} drops down with the convection regime transiting from free to forced convection dominance. This effect is more revealing in the free convection dominant regime compared to the forced convection dominant regime. Further, T_{max} gets larger towards larger k_s in a given convection regime. In the present study, for $k_s = 0.25$ W/m K, there is an overall drop in T_{max} by 36.34 % as Ri_w^* decreases from 25 to 0.1. For the same exercise performed with $k_s = 1$ W/m K, T_{max} decreases by 46.36 %. Further, for $Ri_w^* = 25$, as an example, T_{max} increases by 21.99 % with an increase in k_s to 1 W/m K from 0.25 W/m K.

Role of Aspect Ratio on Peak Temperature of the Channel

The interplay between AR and ε in influencing peak channel temperature is taken up for study. As stated earlier, a larger AR implies a closely spaced channel and a smaller AR means a wider channel. Figure 8 illustrates the variation in T_{max} with AR for three typical values of ε along with the fixed set of input used for study. A sharp increase in T_{max} is noticed, for a given ε, as AR increases from 4 to 20. This effect gets more apparent when one chooses a

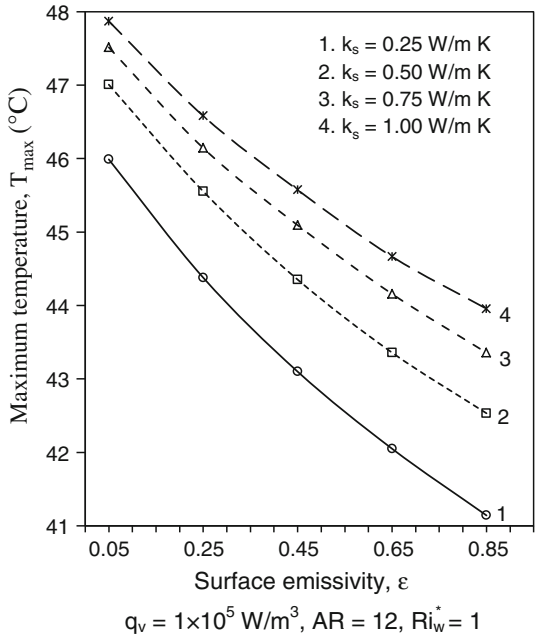

Fig. 6 Effect of surface emissivity on peak channel temperature for different thermal conductivities of wall material

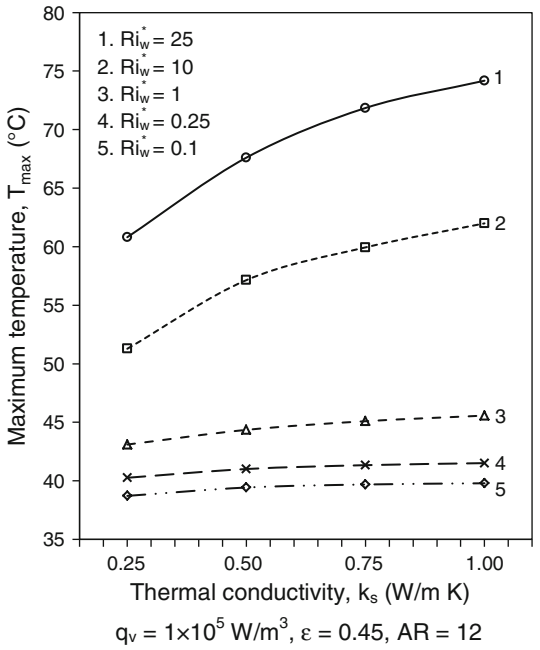

Fig. 7 Effect of thermal conductivity on peak channel temperature in different mixed convection regimes

channel of larger surface emissivity. In the present case, T_{max} increases by 78.4 %, once AR is changed from 4 to 20, for $\varepsilon = 0.05$, while, for $\varepsilon = 0.85$, the same exercise fetches 82.21 % increase in T_{max}. As already stated, an increase in ε brings down T_{max} for a given AR. In the present study, for AR = 12, T_{max} reduces by 8.53 % as ε is varied from 0.05 to 0.85. In view of the above findings, for

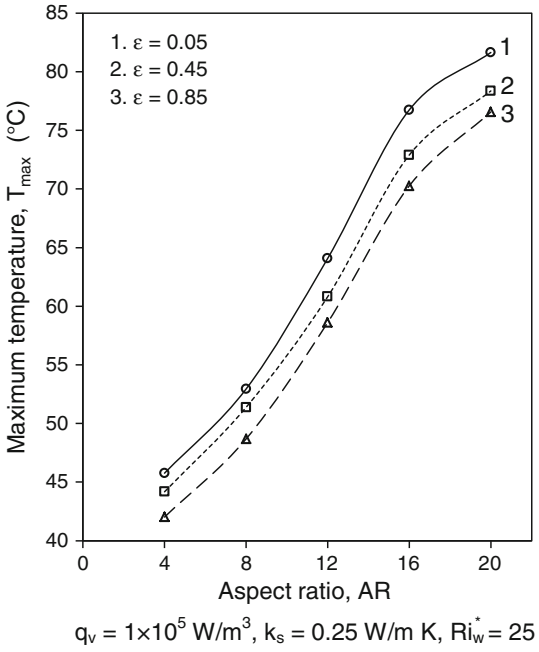

Fig. 8 Effect of aspect ratio on peak channel temperature for different surface emissivities

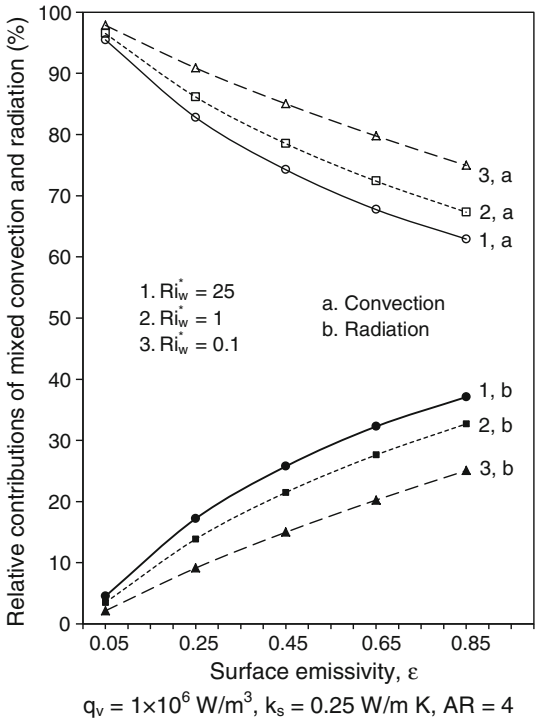

Fig. 9 Relative contributions of convection and radiation in heat dissipation from the channel for different surface emissivities in typical regimes of mixed convection

a given height of the channel, it is never advisable to pack the channel walls too closely, since it increases the load on the cooling system.

Variation of Relative Contributions of Mixed Convection and Radiation with Surface Emissivity in Different Regimes of Mixed Convection

In the present problem, the heat generated in the discrete heat sources in the left wall gets dissipated by the combined modes of mixed convection and radiation. It would be worthwhile to isolate the percentage of heat dissipated by mixed convection and radiation in order to review the complementary roles played by these modes of heat transfer.

The relative contributions from mixed convection and radiation with respect to surface emissivity in three typical regimes of mixed convection are plotted in Fig. 9. As surface emissivity increases, a significant decrease in the contribution from mixed convection is noticed in all the regimes of mixed convection, with a proportionate increase in contribution from radiation. In this example, for $Ri_w^* = 0.1$, i.e., the asymptotic forced convection limit, contribution from radiation increases from 2.1 to 25.1 % with increase in ε to 0.85 from 0.05. A similar exercise for $Ri_w^* = 25$, i.e., asymptotic free convection limit, increases radiative dissipation from 4.5 to 37.1 %. There is a corresponding drop in contribution from mixed convection in both the cases. This observation, yet again, highlights the need to take radiation into reckoning while working with gaseous cooling media. Further, the percentage contribution from radiation is observed to be increasing as one approaches the regime of free convection dominance from that of forced convection dominance. In the present example, for $\varepsilon = 0.45$, contribution from radiation is increasing from 15 to 21.5 % as Ri_w^* increases to 1 from 0.1, while with a further increase in Ri_w^* to 25, radiative dissipation increases to 25.8 %, with an equivalent reduction in the contribution from mixed convection. The above study points out that radiation plays a key role in all the regimes of mixed convection, more so in the free convection dominant regime.

Variation of Relative Contributions of Mixed Convection and Radiation with Aspect Ratio in Different Regimes of Mixed Convection

A study is taken up to comprehend the role of AR in different regimes of convection in influencing the relative contributions of mixed convection and radiation. Figure 10 exhibits the variation of these contributions with AR for three typical values of Ri_w^* along with other input parameters chosen for study. A non-monotonic nature of variation of the contributions with AR is apparent in all the regimes of mixed convection barring pure mixed

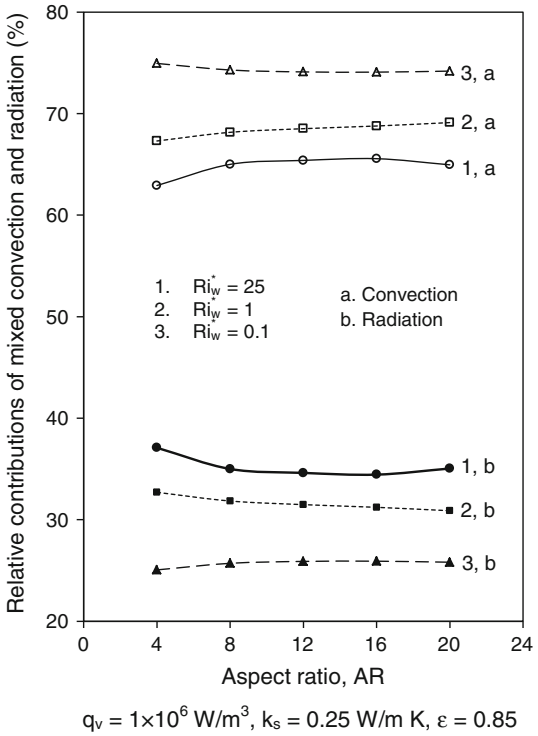

Fig. 10 Relative contributions of convection and radiation in heat dissipation from the channel for different aspect ratios in typical regimes of mixed convection

convection regime ($Ri_w^* = 1$). Convective contribution is noticed to be increasing, although insignificantly, with AR in pure mixed convection regime. In this study, the contribution from convection is increasing from 67.3 % for $AR = 4$ to 69.11 % for $AR = 20$ with comparable decrease in contribution from radiation to 30.89 % from 32.7 %. For asymptotic free convection limit ($Ri_w^* = 25$), convective dissipation increases with increase in AR from 4 to 16. However, with a further increase in AR to 20, a mild drop is observed. Pertaining to asymptotic forced convection limit ($Ri_w^* = 0.1$), convection contribution diminishes, though very slightly, as AR increases from 4 to 16. However, with a further increase in AR to 20, a mild rise is observed. Obviously, there is an analogous change in the role of radiation.

Concluding Remarks

A thorough numerical investigation of the problem of multi-mode heat transfer from a discretely heated vertical channel is made. Exhaustive parametric studies, encompassing the influence of surface emissivity, modified Richardson number, AR and thermal conductivity, are presented. A good emitting surface is observed to decrease the local left wall temperature and increase the local right wall temperature. A substantial drop in the peak channel temperature is observed if the surface coating of the channel is changed from poor emitter ($\varepsilon = 0.05$) to good emitter ($\varepsilon = 0.85$), while the same change in surface coating increases the maximum temperature attained by the right wall. The order of decrease in the local as well as peak temperatures of the walls of the channel with change in mixed convection regime from free convection dominance to forced convection dominance is demonstrated. It is found that there is an increase in peak channel temperature with increase in thermal conductivity on account of increased heat percolation along the channel walls. The study clearly points out that one should avoid close packing of the channel walls as it adversely affects cooling load. A study of relative contributions from convection and radiation in heat dissipation revealed that radiation can not be ignored in all regimes of mixed convection.

References

1. W. Elenbass, Heat dissipation of parallel plates by free convection. Physica **9**, 1–28 (1942)
2. H.C. Agrawal, A variational method for combined free and forced convection in channels. Int. J. Heat Mass Transf. **5**, 439–444 (1962)
3. A. Bar-Cohen, W.M. Rohsenow, Thermally optimum spacing of vertical natural convection cooled parallel plates. ASME J. Heat Transf. **106**, 116–123 (1984)
4. W. Aung, G. Worku, Developing flow and flow reversal in a vertical channel with asymmetric wall temperatures. ASME J. Heat Transf. **108**, 299–304 (1986)
5. J.R. Carpenter, D.G. Briggs, V. Sernas, Combined radiation and developing laminar free convection between vertical flat plates with asymmetric heating. ASME J. Heat Transf. **98**, 95–100 (1976)
6. E.M. Sparrow, S. Shah, C. Prakash, Natural convection in a vertical channel: I. Interacting convection and radiation. II. The vertical plate with and without shrouding. Numer. Heat Transf. **3**, 297–314 (1980)
7. S.H. Kim, N.K. Anand, Laminar heat transfer between a series of parallel plates with surface-mounted discrete heat sources. ASME J. Electron. Packag. **117**, 52–62 (1995)
8. C. Gururaja Rao, C. Balaji, S.P. Venkateshan, Conjugate mixed convection with surface radiation from a vertical plate with a discrete heat source. ASME J. Heat Transf. **123**, 698–702 (2001)
9. C. Gururaja Rao, C. Balaji, S.P. Venkateshan, Effect of surface radiation on conjugate mixed convection in a vertical channel with a discrete heat source in each wall. Int. J. Heat Mass Transf. **45**, 3331–3347 (2002)
10. H. Bhowmik, K.W. Tou, Experimental study of transient forced convection heat transfer from simulated electronic chips. Heat Mass Transf. **41**, 599–605 (2005)
11. S.M. Sawant, C. Gururaja Rao, Conjugate mixed convection with surface radiation from a vertical electronic board with multiple discrete heat sources. Heat Mass Transf. **44**, 1485–1495 (2008)
12. S.M. Aminossadati, B. Ghasemi, A numerical study of mixed convection in a horizontal channel with a discrete heat source in an open cavity. European J. Mech. B/Fluids **28**, 590–598 (2009)

13. V.I. Terekhov, A.L. Ekaid, Laminar natural convection between vertical isothermal heated plates with different temperatures. J. Eng. Thermophys. **20**, 416–433 (2011)
14. H. Sun, R. Li, E. Chénier, G. Lauriat, J. Padet, Optimal plate spacing for mixed convection from an array of vertical isothermal plates. Int. J. Therm. Sci. **55**, 16–30 (2012)
15. A. Sakurai, K. Matsubara, K. Takakuwa, R. Kanbayashi, Radiation effects on mixed turbulent natural and forced convection in a horizontal channel using direct numerical simulation. Int. J. Heat Mass Transf. **55**, 2539–2548 (2012)
16. F.G. Al-Amri, M.A.I. El-Shaarawi, Mixed convection with surface radiation between two asymmetrically heated vertical parallel plates. Int. J. Therm. Sci. **58**, 70–78 (2012)
17. S.E. El-Morshedy, A. Alyan, L. Shouman, Experimental investigation of natural convection heat transfer in narrow vertical rectangular channel heated from both sides. Exp. Therm. Fluid Sci. **36**, 72–77 (2012)
18. R. Li, M. Bousetta, E. Chénier, G. Lauriat, Effect of surface radiation on natural convective flows and onset of flow reversal in asymmetrically heated vertical channels. Int. J. Therm. Sci. **65**, 9–27 (2013)
19. C.D. Dritselis, A.J. Iatridis, I.E. Sarris, N.S. Vlachos, Buoyancy-assisted mixed convection in a vertical channel with spatially periodic wall temperature. Int. J. Therm. Sci. **65**, 28–38 (2013)